sciendo

Green Sciences, 27, 4, 58—64, 10.2478/pjct-2025-0021

Synthesis of Ag/ZIF-67 nanocomposite and its catalytic activity for the reduction of various nitrobenzaldehyde isomers

Sugyeong Jeon[1], Jeong Won Ko[2], Weon Bae Ko[1, 3*]

[1]Department of Convergence Science, Graduate School
[2]Department of Animal Resources Science, Chemistry Major
[3]Department of Chemistry, Sahmyook University, 815 Hwarang-ro, Nowon-gu, Seoul 01795, Republic of Korea
[*]*Corresponding author:* e-mail: kowb@syu.ac.kr

The Ag/ZIF-67 nanocomposite was prepared by the reaction of cobalt nitrate hexahydrate ($Co(NO_3)_2 \cdot 6H_2O$) with 2-methylimidazole and silver nitrate ($AgNO_3$). The morphology and structure of Ag/ZIF-67 nanocomposite were investigated by scanning electron microscopy (SEM), powder X-ray diffraction (XRD), Ultraviolet-visible (UV-vis) spectroscopy, Fourier transform infrared (FT-IR) spectroscopy, and Raman spectroscopy, which indicated that Ag/ZIF-67 composite was successfully synthesized with a rhombic dodecahedron structure. The catalytic activity of the hybrid nanocomposite (Ag/ZIF-67) was investigated toward the reduction of the nitro compounds (2-, 3-, and 4- nitrobenzaldehyde) to their corresponding amino compounds (2-, 3, and 4-aminobenzyl alcohol) in the presence of sodium borohydride (NaBH4) as a reducing agent. The rate for catalytic reduction of nitrobenzaldehyde isomers using Ag/ZIF-67 nanocomposite was in the order: 4- > 2- > 3- nitrobenzaldehyde. The kinetics study showed that the reduction of nitrobenzaldehyde isomers was followed by a pseudo-first-order reaction rate law.

Keywords: Ag/ZIF-67 nanocomposite, catalytic activity, reduction of nitrobenzaldehyde isomers, kinetics study.

Received: 22 April 2024; Accepted: 24 July 2024; Available online: 14.01.2026.

INTRODUCTION

Nitroaromatic compounds are common environmental contaminants and harmful substances to health[1]. Among nitroaromatic compounds, nitrobenzaldehyde is an important intermediate during a number of synthetic processes, causing severe pollution hazards[2]. Also, 4-nitrobenzaldehyde has been widely used as an industrial and medical intermediate for the synthesis of several dyes and pharmaceuticals; it can be found in workplaces and water supplies as a common pollutant[3]. The functionalized aromatic amines derived from the catalytic hydrogenation of nitro compounds are significant in the synthesis of a wide range of beneficial products like pharmaceuticals, dyes, polymers, and herbicides[3, 4, 5].

Several methods have been developed to remove the nitro compounds from wastewater, such as photochemical degradation, adsorption, microbial degradation, membrane distillation, and electrocoagulation[6, 7, 8, 9]. However, the above-mentioned techniques showed some practical limitations like low removal efficiency, high-cost process, and harmful product formation. On the other hand, the catalytic reduction of nitro compounds to amino derivatives is an alternative and emerging process for removing toxic nitro compounds from the environment[10].

The noble metal catalysts such as Au, Pt, Pd, and Ag exhibited high catalytic activity in the reduction of nitro compounds. However, the cost of the catalyst is very expensive and less abundant on Earth. Recently, many studies have reported better catalytic activity for the reaction of nitro compounds using the MOFs structure[11, 12].

Zeolitic Imidazolate Frameworks (ZIFs) are a kind of MOFs where the transition metal (M) cation is coordinated by a bridging imidazole (IM) ligand, with the angle of M-IM-M is 145° [13]. As a kind of ZIFs, ZIF-67, composed of Co^{2+} metal center and 2-methylimidazolate ligand, the structure of ZIF-67 exhibited a cubic crystal symmetry[14]. ZIFs have been widely applied for gas storage, separation, sensors, drug delivery, and catalysis[15, 16, 17, 18, 19, 20]. Sansano et al. revealed that the bimetallic PdCu supported on ZIF-67 catalyst was used in the reduction of 4-nitrophenol at room temperature[21]. Nath et al. discovered that Ag@ZIF-7 effectively catalyzed the reduction of 2-nitrophenol, 4-nitroaniline, and picric acid[22].

In this work, we synthesized the ZIF-67-supported Ag nanoparticles and studied the catalytic reduction of nitrobenzaldehyde isomers from an aqueous solution using Ag/ZIF-67 nanocomposites as a catalyst.

MATERIALS AND METHODS

Materials

Cobalt nitrate hexahydrate ($Co(NO_3)_2 \cdot 6H_2O$), 2-methylimidaozle ($C_4H_6N_2$), 2-nitrobenzaldenyde (2-NBA, $C_7H_5NO_3$), 3-nitrobenzaldehyde (3-NBA, $C_7H_5NO_3$), 4-nitrobenzaldehyde (4-NBA, $C_7H_5NO_3$), silver nitrate ($AgNO_3$), ethanol (C_2H_5OH), and methanol (CH_3OH) were purchased from Sigma-Aldrich (USA) and Daejung chemicals (Korea). All the chemicals were used without further purification.

Characterization

The crystalline properties of the synthesized ZIF-67 and Ag/ZIF-67 nanocomposites were investigated by powder X-ray diffraction (XRD, Bruker, D8 Advance, Germany) analysis with Cu-Kα radiation ($\lambda = 1.541$ nm) within a 2θ range of 5–90°. The ZIF-67 and hybrid Ag combined with ZIF-67 nanocomposite were confirmed by Raman spectroscopy at 532 nm wavelength (BWTEK i-Raman Plus, USA). The morphology of the catalyst was observed by using field emission scanning electron microscopy (FE-SEM, EDS, TESCAN MIRA 3, Czech Republic) at an acceleration voltage of 15 kV. The functional group of the catalyst was analyzed using Fourier

transform infrared spectroscopy (FT-IR, Thermo Fisher Scientific Nicolet Continuum IR Microscope, USA). The reduction of nitro compounds was confirmed by ultraviolet-visible (UV-vis) spectroscopy (Lambda 365, Perkin Elmer, USA).

Synthesis of ZIF-67 nanoparticles

According to literature[23], cobalt nitrate hexahydrate (1.45 g) and 2-methylimidazole (1.64 g) were dissolved in 80 ml of methanol/ethanol solution (1:1, v/v), respectively. The above two solutions were mixed and stirred for 30 min and left for 24 h. After the reaction was finished, the precipitate was rinsed several times with methanol and collected after centrifugation to acquire the ZIF-67 product.

Synthesis of Ag/ZIF-67 nanocomposite

For the preparation of Ag/ZIF-67 nanocomposite, ZIF-67 was heated at 100 °C under a vacuum condition for 5 h to obtain an optimally dried solid-state sample. The ZIF-67 (0.24 mmol) was dissolved in 11 mL of ethanol and stirred for 30 min. After that, the $AgNO_3$ (0.03 mmol) in ethanol solution was added to ZIF-67 in ethanol solution and vigorously stirred for 5 h. After stirring, the Ag^+/ZIF-67 product was obtained by centrifugation. The product was dried overnight in an oven at 60 °C. For the reduction of Ag^+/ZIF-67, 4 mL of $NaBH_4$ (0.3 mmol) in ethanol solution was added to Ag^+/ZIF-67 in ethanol solution. The mixture was stirred for 30 min, and the obtained purple-black precipitation was washed with ethanol. The precipitate was dried at 60 °C in an oven.

Reduction of various nitrobenzaldehyde isomers

The reduction of nitro compounds was monitored, such as 2-, 3-, and 4-NBA, under the same reaction conditions of concentration for each nitro compound (0.05 mM), $NaBH_4$ (2.7 mM), and catalyst dosage (0.1 g/L) at room temperature. The catalytic reduction was measured through UV-vis spectrophotometry at constant time intervals. The UV-vis spectrophotometry data confirmed by the absorption peaks of the solution at a constant time. The absorbance peaks of 2-, 3-, 4-NBA appeared at 256 nm, 233 nm, and 268.5 nm, respectively. The nitrobenzaldehyde was reduced to alcohol with sodium borohydride ($NaBH_4$). After adding $NaBH_4$ solution, the UV spectra showed the 2-, 3-, 4- nitrobenzylalcohol at 266 nm, 269 nm, 276.5 nm. After the catalytic reaction, the 2-aminobenzylalcohol (282.5 nm), 3-aminobenzylalcohol (272 nm), and 4-aminobenzylalcohol (237 nm and 283 nm) were confirmed by UV-vis spectroscopy[1, 24].

RESULTS AND DISCUSSIONS

Characterization of Ag/ZIF-67 nanocomposite

The XRD results of ZIF-67 and Ag/ZIF-67 nanocomposite were shown in Figure 1(a). For ZIF-67, the XRD peaks observed at 2θ = 7.35°, 10.39°, 12.73°, 14.71°, 16.45°, and 18.03° correspond to the (011), (002), (112), (022), (013), and (222) planes of the sodalite structure. The characteristic peaks of Ag and ZIF-67 could be found in Ag/ZIF-67 nanocomposite. The XRD peak values of Ag were observed at 2θ = 38.1° and 44.4°, which correspond to the (111) and (200) planes of the cubic phase (JCPDS No. 87-717)[25, 26]. The XRD result demonstrated that Ag/ZIF-67 nanocomposite was successfully synthesized, and the incorporated Ag did not change the structure of ZIF-67.

The crystallite size of Ag in the synthesized Ag/ZIF-67 nanocomposite was calculated using the Scherrer formula.

$$D = \frac{K\lambda}{\beta\cos\theta} \quad (1)$$

Where D is the crystallite size, K is the Scherrer constant, λ is the X-ray wavelength (CuKα=1.541 Å), β is the full width at half maximum (FWHM) intensity of the XRD peak in radians, and θ is the Bragg angle. The average crystallite size of the Ag was calculated to be 14.4 nm (Table 1).

Table 1. Estimation of crystallite size for Ag nanoparticle in Ag/ZIF-67 nanocomposite using the Scherrer Equation

Peak	2θ (degree)	FWHM (°)	Crystallite size (nm)
(111)	38.2	0.469	17.9
(200)	44.3	0.784	10.9
Average (Ag)			14.4

The FT-IR spectra of ZIF-67 and Ag/ZIF-67 nanocomposite are shown in Figure 1(b). The vibrational bands in the range of 400–4000 cm^{-1} were obtained for the sample. The peaks were mainly caused by the organic ligand, which is 2-methylimidazole. The absorption bands of 600–1600 cm^{-1} are attributed to stretching and bending

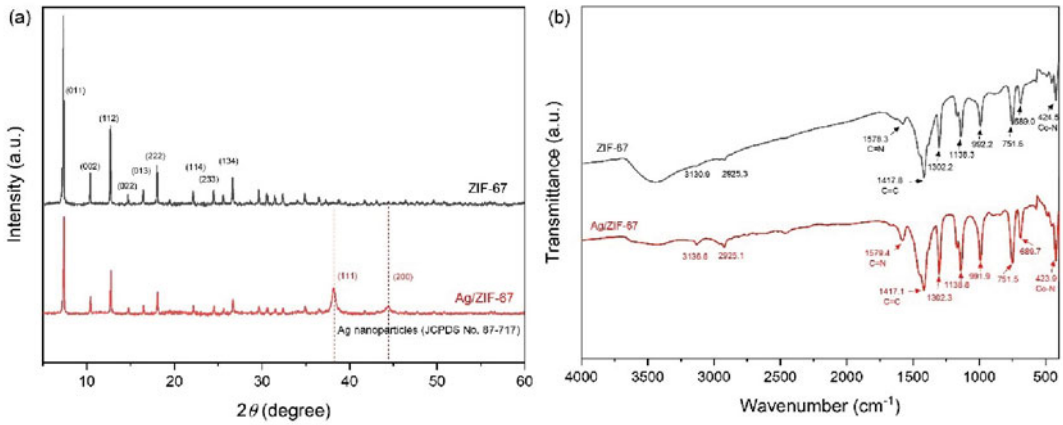

Figure 1. (a) XRD patterns and (b) FT-IR spectra of synthesized ZIF-67 and Ag/ZIF-67 nanocomposite

modes of the imidazole ring in Ag/ZIF-67 nanocomposite. The bands at 2925.3 cm^{-1} and 3130.9 cm^{-1} in ZIF-67 and 2725.1 cm^{-1} and 3136.6 cm^{-1} in Ag/ZIF-67 nanocomposite can be associated with the stretching mode from the aliphatic methyl group and aromatic ring. The band at 424.5 cm^{-1} can be attributed to Co-N stretching mode. It also indicated that the presence of silver nanoparticles did not change the structure of ZIF-67.

Figure 2 shows the Raman spectra of ZIF-67 and Ag/ZIF-67 nanocomposite in the range of 300–1200 cm^{-1}. The peaks at 463, 509, 675 cm^{-1} were associated with ZIF-67, including the Co-N bond at 463 cm^{-1}, and the vibrational mode of the 2-methylimidazole ligand at 675 cm^{-1} [27]. The peak of ZIF-67 at 675 cm^{-1} moved into a lower shift compared to the peak of Ag/ZIF-67 nanocomposite at 668 cm^{-1} in Raman spectra.

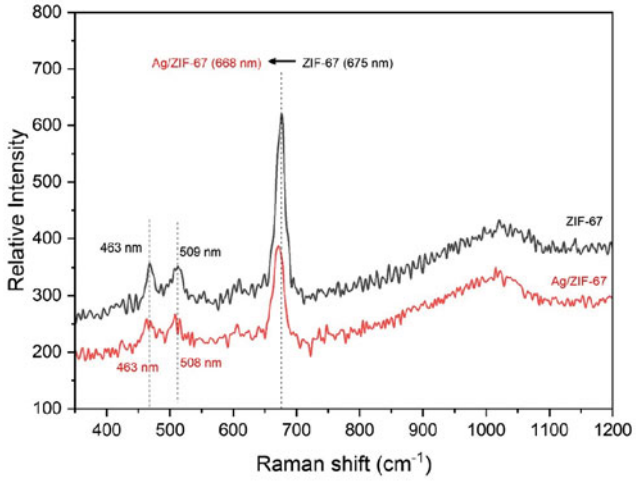

Figure 2. Raman spectra of synthesized ZIF-67 and Ag/ZIF-67 nanocomposite

The UV-vis spectra of ZIF-67 and Ag/ZIF-67 nanocomposite are shown in Figure 3(a). The absorbance peak of the ZIF-67 was observed at 595 nm. The adsorption peak of the Ag/ZIF-67 nanocomposite was moved to 600 nm, due to the presence of Ag nanoparticles on the ZIF-67 surface. The Eg according to Tauc's plot was calculated to be 1.98 and 1.94 eV for ZIF-67 and Ag/ZIF-67 nanocomposite in Figure 3(b). These results confirmed the optical properties of ZIF-67 and Ag nanoparticles on the ZIF-67 and their performance in the catalytic process.

$$\alpha h\nu = A[h\nu - Eg]^{k} \quad (2)$$

Where α is the absorption coefficient, h is Planck constant, ν is the light frequency, A is a characteristic constant, Eg is the apparent optical bandgap of the material, and k is a constant associated with electronic transition types (for direct allowed transition: k = 1/2)[28].

The SEM images of ZIF-67 and Ag/ZIF-67 nanocomposite are shown in Figure 4(a) and (b). The SEM image of the ZIF-67 shows rhombic-dodecahedral morphology in Figure 4(a). The morphology of ZIF-67 in Ag/ZIF-67 nanocomposite has slightly shrunk due to the decomposition of imidazole ligands during the synthesis process. Ag nanoparticles were dispersed on the surface of ZIF-67 in Figure 4(b).

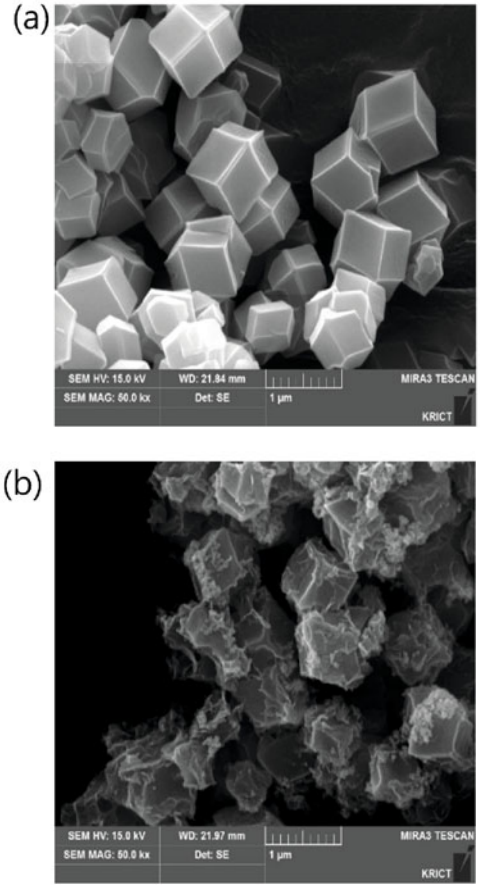

Figure 4. SEM images of the (a) ZIF-67 and (b) Ag/ZIF-67 nanocomposite

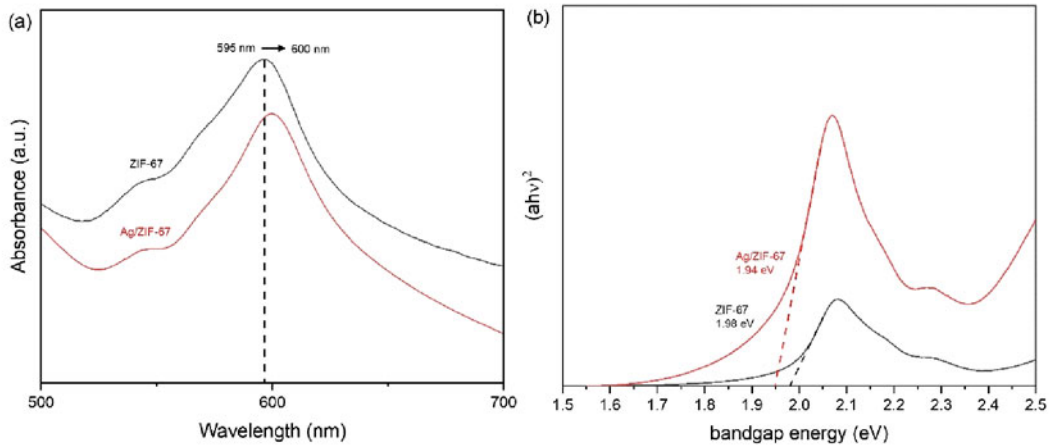

Figure 3. (a) UV-vis spectra and (b) Tauc's plot for the band energy of the ZIF-67 and Ag/ZIF-67 nanocomposite

Catalytic reduction of nitrobenzaldehyde isomers

The reduction of 2-, 3-, 4-nitrobenzaldehyde was studied using $NaBH_4$ as the reducing agent and ZIF-67 and Ag/ZIF-67 nanocomposite as catalysts. It was observed that the reduction of the aldehyde group to the alcohol group was previously happened before the reduction of the nitro group. Therefore, within a minute, only the reduction of the aldehyde group was observed; thus, the spectra showed the formation of 2-, 3-, 4-nitrobenzylalcohol, respectively. As the reduction proceeded, the UV-vis spectra displayed peaks of absorption maximum corresponding to both the hydrogenated products of nitro moieties of the nitrobenzaldehyde isomers. Consequently, 2-, 3-, 4-aminobenzylalcohol showed bands at 282.5 nm (2-aminobenzylalcohol), 272 nm (3-aminobenzylalcohol), and 237 nm and 283 nm (4-aminobenzylalcohol), respectively (Fig. 5).

Kinetic study for catalytic reduction of nitrobenzaldehyde isomers

As the constant concentration of $NaBH_4$ added to the solution of nitrobenzaldehyde isomers, it was considered to be a fixed concentration of $NaBH_4$ during the reaction was performed[29]. So the reaction kinetics could be considered as pseudo-first order with respect to the reduction of nitrobenzaldehyde isomers. The apparent rate constant (k) for a pseudo-first-order reaction could be defined through the equation:

$$\ln\left(\frac{C}{C_0}\right) = -kt \quad (3)$$

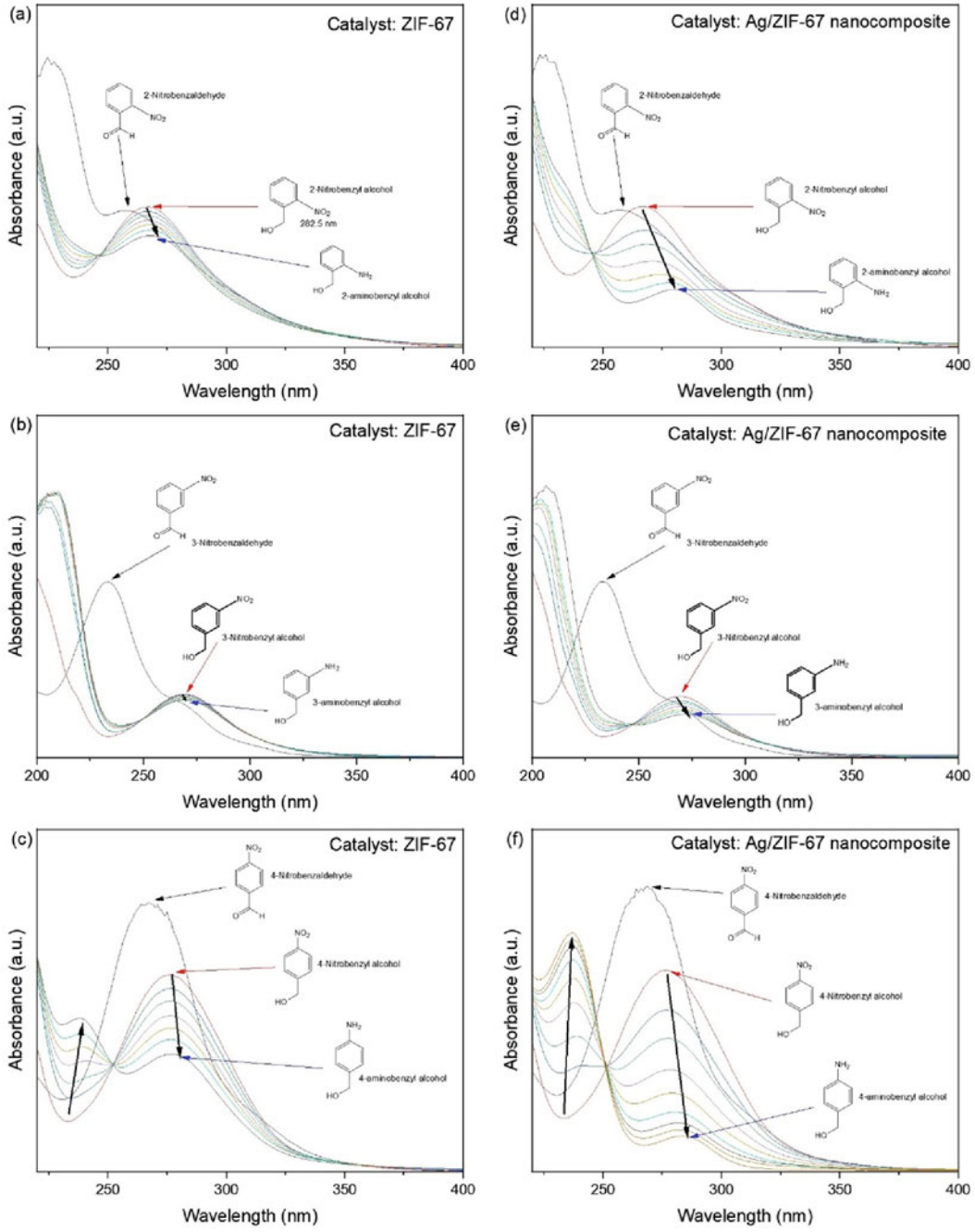

Figure 5. UV-vis absorption spectra of reduction of (a, d) 2-nitrobenzaldehyde (b, e) 3- nitrobenzaldehyde, and (c, f) 4- nitrobenzaldehyde by a ZIF-67 and Ag/ZIF-67 nanocomposite

Where C_0 is the concentration of the constant at an initial time at t=0, C is the concentration of the reaction at a specific time at t, and k is the first-order rate constant[30]. The linear behavior of the curves confirms that the reduction of nitro compounds, which were 2-, 3-, 4- nitrobenzaldehyde, followed a pseudo-first-order reaction rate law, as can be observed from Figure 6(a) and (b). The rate constant k represents a value associated with the reaction rate. In reduction reactions, compounds experience a process where they accept electrons or receive hydrogen. Therefore, a negative value of the rate constant k indicates the progression of a reduction reaction. The calculated k values obtained using ZIF-67 catalysts are as follows: –0.038 s^{-1} for 2-nitrobenazaldehyde, –0.016 s^{-1} for 3-nitrobenazaldehyde, and –0.085 s^{-1} for 4- nitrobenazldehyde. Also, when Ag/ZIF-67 nanocomposite was used as the catalyst, the calculated rate constants k values were obtained as –0.151 s^{-1}, –0.057 s^{-1}, and –0.242 s^{-1} for 2-, 3-, 4- nitrobenzaldehyde, respectively. The reduction reactions of nitrobenzaldehyde isomers using ZIF-67 and Ag/ZIF-67 nanocomposite showed the same kinetic order. The results showed reduction efficiency of nitro benzaldehyde isomers in the order, 3-NBA < 2-NBA < 4-NBA. In the results, the order of reduction rate was para > ortho > meta. This trend is attributed to the stronger mesomeric and electron-withdrawing properties of the aldehydic group.

Reusability tests of the Ag/ZIF-67 nanocomposite as a catalyst

Recycling of heterogeneous catalysts is becoming increasingly important in industrial applications. Figure 7 presents the results of the reusability tests of the Ag/ZIF-67 nanocomposite in the reduction of 4-nitrobenzaldehyde over five consecutive reaction cycles under identical conditions. The results show that the catalytic activity of Ag/ZIF-67 decreased only slightly, from 83.06% in the first run to 80.65% after the fifth cycle, indicating good stability and reusability of the catalyst.

Mechanism for the reduction of nitrobenzaldehyde isomers by Ag/ZIF-67 nanocomposite as a catalyst

The mechanism for the reduction of nitrobenzaldehyde isomers with $NaBH_4$ in an aqueous system is shown in Figure 8. This reduction process involves the reduction of nitro to amino groups, achieved by $NaBH_4$ as a reducing agent. It is well established that reduction from nitro to amino compounds cannot be reduced by using $NaBH_4$. The electron transfer occurs from BH_4^- ions, which act as electron donors in the reduction of nitro compounds. In the presence of a catalyst, BH_4^- ions are adsorbed on the surface of the catalyst. This leads to the initiation of electron discharge from the donor of BH_4^- ions. The discharged electrons are subsequently transferred

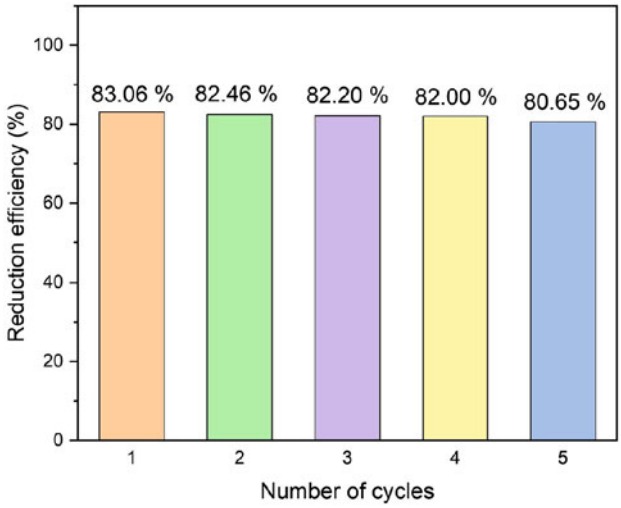

Figure 7. Reusability tests of the Ag/ZIF-67 nanocomposite for the reduction of 4-nitrobenzaldehyde

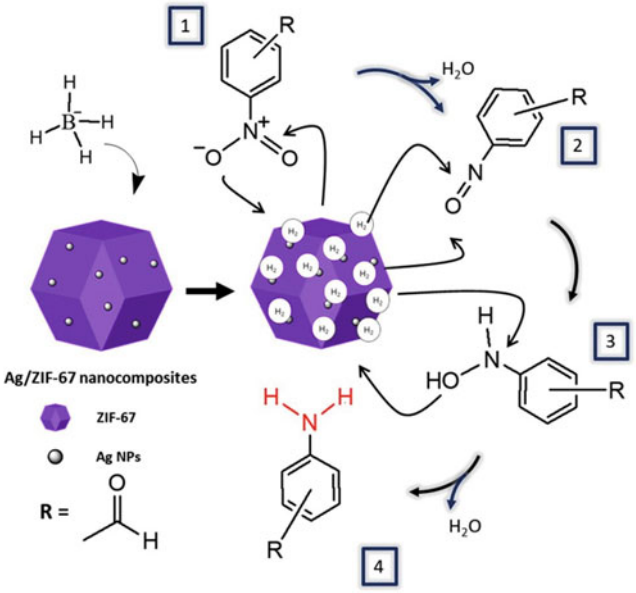

Figure 8. Reduction mechanism of nitrobenzaldehyde isomers

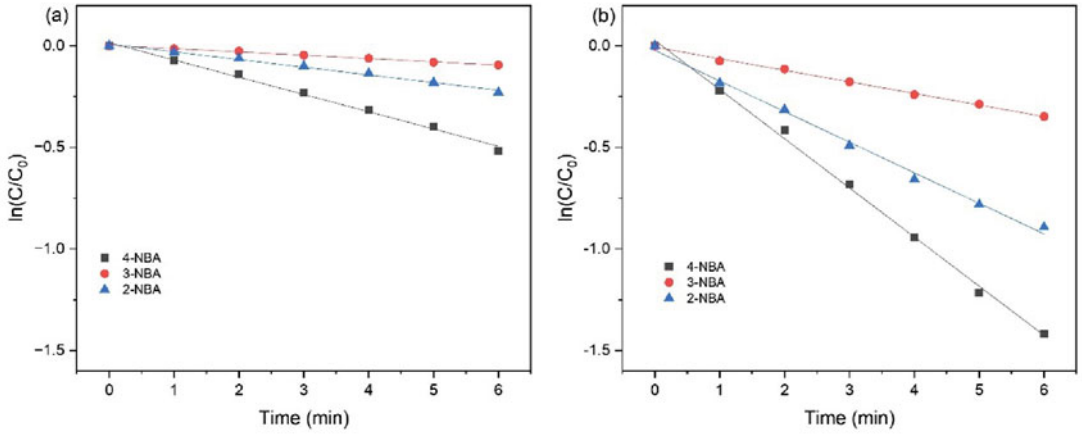

Figure 6. Kinetics study for the reduction of nitrobenzaldehyde isomers using (a) ZIF-67 and (b) Ag/ZIF-67 nanocomposite

through the metal catalyst to the nitro compound in the reduction process. The aqueous medium consists of H^+ ions for the complete reduction of nitro to amino compounds[21, 31, 32].

CONCLUSIONS

The synthesized ZIF-67 and Ag/ZIF-67 nanocomposite were employed as catalysts for the reduction of 2-, 3-, and 4-nitrobenzaldehyde in aqueous solution using $NaBH_4$ as a reducing agent. The Ag/ZIF-67 nanocomposite exhibited significantly higher catalytic performance compared to pristine ZIF-67. For ZIF-67, the apparent rate constants (k) for the reduction of 2, 3-, and 4-nitrobenzaldehyde were determined to be 0.038 s^{-1}, 0.016 s^{-1}, and 0.085 s^{-1}, respectively. Under identical conditions, Ag/ZIF-67 showed considerably higher rate constants of 0.151 s^{-1}, 0.057 s^{-1}, and 0.242 s^{-1} for the same substrates. These results confirm the superior catalytic efficiency of Ag/ZIF-67 in comparison to ZIF-67 alone. At constant $NaBH_4$ concentration, the reduction reactions followed pseudo-first-order kinetics. The overall reduction efficiency of the nitrobenzaldehyde isomers using ZIF-67 and Ag/ZIF-67 as catalysts followed the order: 4-NBA > 2-NBA > 3-NBA.

ACKNOWLEDGEMENT

This study was supported by research funding from Sahmyook University, South Korea.

LITERATURE CITED

1. Riaz, M., Khan, N., Khan, S.A., Ahmad, Z., Khan, M.A., Iqbal, M., Hemeg, H.A., Bakhsh, E.M. & Khan, S.B. (2022). Enhanced catalytic reduction/degradation of organic pollutants and antimicrobial activity with metallic nanoparticles immobilized on copolymer modified with NaY zeolite films. *J. Mol. Liq.*, 359,119246–119270. DOI: 10/1016/j.molliq.2022.119246.

2.Yuan, F., Halawa, M.I., Ma, X., Abdussalam, A., Lou, B. & Xu, G. (2020). Electrochemiluminescence of $Ru(bpy)_3^{2+}$/ Oxamic Hydrazide and its Application for Selective Detection of 4-Nitrobenzaldehyde. *Chem. Electro. Chem.* 7, 4239–4244. DOI: 10.1002/celc.202001140.

3.Santos, A.S.G.G., Orge, C.A., Soares, O.S.G.P. & Pereira, M.F.R. (2020). 4-Nitrobenzaldehyde removal by catalytic ozonation in the presence of CNT. *J. Water Proc. Engin.* 38,101573–101580. DOI: 10.1016/j.jwpe.2020.101573.

4. Yildiz, S., Sahiner, M. & Sahiner, N. (2015). Ionic liquid hydrogel templates: bulk gel, cryogel, and microgel to be used for metal nanoparticle preparation and catalysis. *Eur. Polym. J.*, 70, 66–78. DOI: 10.1016/j.eurpolymj.2015.07.005.

5. Khorshidi, A. & Ghorbannezhad, B. (2017). A highly effective Ag–RANEY® nickel hybrid catalyst for reduction of nitrofurazone and aromatic nitro compounds in aqueous solution. *RSC Adv.*, 7, 29938–29943. DOI: 10.1039/c7ra04343k.

6. Ahmad, W., Singh, A., Jaiswal, K.K. & Gupta, P. (2021). Green synthesis of photocatalytic TiO_2 nanoparticles for potential application in photochemical degradation of ornidazole. *J. Inorg. Organomet. Polym. Mater.* 31, 614–623. DOI:10.1007/ s10904-020-01703-6.

7. Min, J., Xu, L., Fang, S., Chen, W. & Hu, X. (2020). Microbial degradation kinetics and molecular mechanism of 2, 6-dichloro-4-nitrophenol by a *Cupriavidus* strain. *Environ. Pollut.* 258, 113703–113712. DOI: 10.1016/j.envpol.2019.113703.

8. Ramos, R.L., Martins, M.F., Lebron, Y.A., Moreira,V.R., Reis, B.G., Grossi, L.B. & Amaral, M.C.S. (2021). Membrane distillation process for phenolic compounds removal from surface water. *J. Environ. Chem. Eng.* 9, 105588–105596. DOI: 10.1016/j.jece.2021.105588.

9. Modirshahla, N., Behnajady, M.A. & Mohammadi-Aghdam, S. (2008). Investigation of the effect of different electrodes and their connections on the removal efficiency of 4-nitrophenol from aqueous solution by electrocoagulation. *J. Hazard. Mater.*, 154, 778–786. DOI: 10.1016/j.jhazmat.2007.10.120.

10. Neal, R.D., Inoue, Y., Hughes, R.A. & Neretina, S. (2019). Catalytic reduction of 4-nitrophenol by gold catalysts: the influence of borohydride concentration on the induction time. *J. Phys. Chem. C*, 123, 12894–12901. DOI: 10.1021/acs. jpcc.9b02396.

11. Ramu, A.G., Kumari, M.A., Elshikh, M.S., Alkhamis, H.H., Alrefaei, A.F. & Choi, D. (2021). A facile and green synthesis of CuO/NiO nanoparticles and their removal activity of toxic nitro compounds in aqueous medium. *Chemosphere*, 271, 129475–129483, DOI: 10.1016/j.chemosphere.2020.129475.

12. Navalón, S., Álvaro, M., Dhakshinamoorthy, A. & García, H. (2019). Encapsulation of metal nanoparticles within metal–organic frameworks for the reduction of nitro compounds. *Molecules*, 24, 3050–3072. DOI: 10.3390/molecules24173050.

13. Bibi, S., Pervaiz, E. & Ali, M. (2021). Synthesis and applications of metal oxide derivatives of ZIF-67: a mini-review, *Chem. Pap.*, 75, 2253–2275. DOI:10.3390/molecules24173050.

14. Mu, L., Liu, B., Liu, H., Yang, Y., Sun, C. & Chen, G. (2012). A novel method to improve the gas storage capacity of ZIF-8. *J. Mater. Chem.* 22, 12246–12252. DOI: 10.1039/ C2JM31541F.

15. Zhong, G., Liu, D. & Zhang, J. (2018). The application of ZIF-67 and its derivatives: adsorption, separation, electrochemistry and catalysts. *J. Mater. Chem. A,* 6, 1887–1899. DOI: 10.1039/C7TA08268A.

16. Matatagui, D., Sainz-Vidal, A., Gràcia, I., Figueras, E., Cané, C. & Saniger, J.M. (2018). Chemoresistive gas sensor based on ZIF-8/ZIF-67 nanocrystals. *Sens. Actuators B: Chem.,* 274, 601–608. DOI: 10.1016/j.snb.2018.07.137.

17. Wang, L., Zhu, H., Shi, Y., Ge, Y., Feng, X., Liu, R. & Wang, L. (2018). Novel catalytic micromotor of porous zeolitic imidazolate framework-67 for precise drug delivery. *Nanoscale*, 10, 11384–11391. DOI: 10.1039/C8NR02493F.

18. Meng, Y., Zhang, L., Jiu, H., Zhang, Q., Zhang, H., Ren, W. & Li, D. (2019). Construction of g-C3N4/ZIF-67 photocatalyst with enhanced photocatalytic CO_2 reduction activity. *Mater. Sci. Semicond. Process,* 95, 35–41. DOI: 10.1016/j. mssp.2019.02.010.

19. Shi, F., Ding, M., Tong, H., Yang, Y., Zhang, J., Wang, L. & Huo, Y. (2022). Photoelectrocatalytic sterilization on thorn-like ZIF-67/ZnO hybrid photoanodes. *J. Environ. Chem. Eng.,* 10, 107385–107393. DOI: 10.1016/j.jece.2022.107385.

20. Zhang, M., Liu, Q., Sun, L., Su, H. & Qi, C. (2020). Synthesis of high efficient and stable Au@ ZIF-8 with difference particle size for chemselective hydrogenation of nitro compounds. *Catal. Lett.,* 150, 438–449. DOI: 10.1007/s10562-019-02963-9.

21. Gholinejad, M., Naghshbandi, Z. & Sansano, J.M. (2022). Zeolitic imidazolate frameworks-67 (ZIF-67) supported PdCu nanoparticles for enhanced catalytic activity in Sonogashira-Hagihara and nitro group reduction under mild conditions. *Mol. Catal.* 518, 112093–112103. DOI: 10.1016/j.mcat.2021.112093.

22. Malik, A. & Nath, M. (2020). Synthesis of Ag/ZIF-7 by immobilization of Ag nanoparticles onto ZIF-7 microcrystals: A heterogeneous catalyst for the reduction of nitroaromatic compounds and organic dyes. *J. Environ. Chem. Eng.* 8, 104547–104561. DOI: 10.1016/j.jece.2020.104547.

23. Meng, W., Wen, Y., Dai, L., He, Z. & Wang, L. (2018). A novel electrochemical sensor for glu cose detection based on Ag@ ZIF-67 nanocomposite. *Sens. Actuators B: Chem.* 260, 852–860. DOI: 10.1016/j.snb.2018.01.109.

24. Baba, A., Ouahbi, H., Hassine, A., Sebti, J., Laasri, L. & Sebti, S. (2018). Efficient reduction of aromatic nitro

compounds catalyzed by nickel chloride supported on natural phosphate. *Mediterr. J. Chem.* 7, 317–327. DOI: 10.13171/MJC751911281520SS.

25. Saghir, S. & Xiao, Z. (2021). Synthesis of novel Ag@ ZIF-67 rhombic dodecahedron for enhanced adsorptive removal of antibiotic and organic dye. *J. Mol. Liq.,* 328, 115323–115334. DOI: 10.1016/j.molliq.2021.115323.

26. Dong, Y., Duan, C., Sheng, Q. & Zheng, J. (2019). Preparation of Ag@ zeolitic imidazolate framework-67 at room temperature for electrochemical sensing of hydrogen peroxide. *Analyst*, 144, 521–529. DOI: 10.1039/C8AN01641K.

27. Ma, L., Zhang, X., Ikram, M., Ullah, M., Wu, H. & Shi, K. (2020). Controllable synthesis of an intercalated ZIF-67/EG structure for the detection of ultra trace Cd^{2+}, Cu^{2+}, Hg^{2+} and Pb^{2+} ions. *Chem. Eng. J.* 395, 125216–125227. DOI: 10.1016/j.cej.2020.125216.

28. Kohantorabi, M., Giannakis, S., Moussavi, G., Bensimon, M., Gholami, M.R. & Pulgarin, C. (2021). An innovative, highly stable Ag/ZIF-67@ GO nanocomposite with exceptional peroxymonosulfate (PMS) activation efficacy, for the destruction of chemical and microbiological contaminants under visible light. *J. Hazard. Mater.* 413, 125308–125325. DOI: 10.1016/j.jhazmat.2021.125308.

29. Shin, K.S., Cho, Y.K., Choi, J.Y. & Kim, K. (2012). Facile synthesis of silver-deposited silanized magnetite nanoparticles and their application for catalytic reduction of nitrophenols. *Appl. Catal. A: Gen. 413*, 170–175. DOI: 10.1016/j.apcata.2011.11.006.

30. Goyal, A., Bansal, S. & Singhal, S. (2014). Facile reduction of nitrophenols: Comparative catalytic efficiency of MFe_2O_4 (M= Ni, Cu, Zn) nano ferrites. *Int. J. Hydrog. Energy,* 39, 4895–4908. DOI: 10.1016/j.ijhydene.2014.01.050.

31. Shah, M.T., Balouch, A., Pathan, A.A., Mahar, A.M., Sabir, S., Khattak, R. & Umar, A.A. (2017). SiO_2 caped Fe_3O_4 nanostructures as an active heterogeneous catalyst for 4-nitrophenol reduction. *Microsyst. Technol.* 23, 5745–5758. DOI: 10.1007/s00542-017-3431-8.

32. Samuel, M.S., Bhattacharya, J., Parthiban, C., Viswanathan, G. & Singh, N.D.P. (2018). Ultrasound-assisted synthesis of metal organic framework for the photocatalytic reduction of 4-nitrophenol under direct sunlight. *Ultrason. Sonochem. 49*, 215–221. DOI: 10.1016/j.ultsonch.2018.08.004.